

Piezoelectric-Based Energy Conversion and Storage Materials

Sihui Wang¹, Lei Wen², Xiaopeng Gong¹, Ji Liang³, Xinggang Hou^{4,*} and Feng Hou^{3,*} 

¹ School of Aeronautics and Astronautics, Tianjin Sino-German University of Applied Sciences, Tianjin 300350, China; wangsihui@tju.edu.cn (S.W.); gongxiaopeng@stud.tjut.edu.cn (X.G.)

² Shenyang National Laboratory for Materials Science, Institute of Metal Research, Chinese Academy of Sciences, 72 Wenhua Road, Shenyang 110016, China; leiwen@imr.ac.cn

³ School of Materials Science and Engineering, Tianjin University, Tianjin 300072, China; liangji@tju.edu.cn

⁴ Applied Physics Department, College of Physics and Materials Science, Tianjin Normal University, Tianjin 300350, China

* Correspondence: hou226@tjnu.edu.cn (X.H.); houf@tju.edu.cn (F.H.); Tel.: +86-138-2096-3375 (F.H.)

Abstract: The world's energy crisis and environmental pollution are mainly caused by the increase in the use of fossil fuels for energy, which has led scientists to investigate specific cutting-edge devices that can capture the energy present in the immediate environment for subsequent conversion. The predominant form of energy is mechanical energy; it is the most prevalent energy in the environment and can be harvested for conversion into useful, electrical energy. Compared with electromagnetic, electrostatic, magnetostrictive, dielectric elastomer and frictional electric transducers, piezoelectric transducers have higher high electrical and mechanical constants, large electromechanical coupling coefficients, high dielectric numbers and low losses and are currently the most dominant method of mechanical energy acquisition. Therefore, the research of piezoelectric transducers has received great attention from the scientific community. This paper reviews the research progress of piezoelectric energy acquisition technology. The main objective of this paper is to compile, discuss and summarize the recent literature on piezoelectric energy harvesting materials and applications. Piezoelectric catalytic materials, piezoelectric supercapacitors (SCs), piezoelectric self-charging devices and piezoelectric electrochemical energy storage are mainly introduced. This review briefly introduces the recent advances in piezoelectric-based catalysts and electrochemical energy storage, concentrating on the attributes of various piezoelectric materials and their uses.

Keywords: piezoelectric energy acquisition; piezoelectric-based catalysts; electrochemical energy storage



Citation: Wang, S.; Wen, L.; Gong, X.; Liang, J.; Hou, X.; Hou, F.

Piezoelectric-Based Energy Conversion and Storage Materials. *Batteries* **2023**, *9*, 371. <https://doi.org/10.3390/batteries9070371>

Academic Editor: Federico Baronti

Received: 25 May 2023

Revised: 25 June 2023

Accepted: 28 June 2023

Published: 10 July 2023



Copyright: © 2023 by the authors. Licensee MDPI, Basel, Switzerland. This article is an open access article distributed under the terms and conditions of the Creative Commons Attribution (CC BY) license (<https://creativecommons.org/licenses/by/4.0/>).

1. Introduction

Piezoelectric materials are the key functional components in energy-related fields, such as photo/electro catalysis, electrode materials for secondary batteries and supercapacitors. In particular, piezoelectric materials are able to generate an electric field in response to mechanical deformation. The applications take advantage of the direct or reverse piezoelectric effects. Piezoelectric materials have been extensively explored for energy harvesting and storage devices because they can transform irregular and low-frequency mechanical vibrations into electricity [1–3]. Piezoelectric films are wearable and flexible energy generators, due to their superior mechanical and piezoelectric capabilities [4–7].

Furthermore, the piezoelectric effect leads to piezoelectric polarization. The piezoelectric materials have a noticeable effect in an active mode, providing a voltage signal in response to applied force/pressure. The piezoelectric effect is a new, fundamental mechanism that allows the comingling of energy conversion and storage processes into a single step. This process is as follows: mechanical energy is converted and simultaneously stored as electrochemical energy [8]. For example, a highly porous film can act as an effective piezo separator for enhanced self-charging piezoelectric ceramics (SCPCs). Notably, the device can be stabilized, and charge transfer resistance is lowered due to the porous structure.

Additionally, the absorbent structure makes a self-charging action caused by the piezo potential possible, which can prevent substantial capacity deterioration [9].

Moreover, piezoelectric effects successfully realize mechanical energy harvesting and energy conversion [10–13]. Piezoelectric materials can transform mechanical motion in the environment into electrical energy. These mechanical motions cover various daily aspects, such as human motion, rotating tires, mechanical triggering, wind and waves, etc., [14]. These piezoelectric materials have applications in lithium–sulfur (Li-S) batteries and emerging applications such as electric vehicles (EVs), drones and unmanned aerial vehicles, due to the unprecedented theoretical capacity and low cost of piezoelectric materials [15]. The piezoelectric materials may resist the shuttling process. By creating unstable interfaces at both electrodes and removing the sulfur cathode’s active material, the shuttling process results in self-discharge and reduces cyclability. Beyond its primary purpose of preventing direct contact between the two electrodes, the piezoelectric effect can significantly reduce PS migration because the separator can regulate the movement of carrier ions and byproducts.

Piezoelectric components have attracted much attention lately, for their potential to harvest energy from ambient vibration. Due to the piezoelectric element’s meagre power output, energy storage devices are required for sporadic use. Supercapacitors and rechargeable batteries are the leading energy storage technologies taken into account. The collected energy must be exchanged and stored to integrate energy harvesting and storage devices, until sufficient power can be applied to electric machines and systems. The energy harvesting of mechanical vibrations is suitable for structural health monitoring.

At present, piezoelectric ceramics are widely used in the energy field, and there are not many researches on piezoelectric energy storage. Due to their unique, structural properties, piezoelectric ceramics have a good application potential in energy storage, including piezoelectric catalysis, piezoelectric applications in batteries and piezoelectric applications in supercapacitors (Figure 1). According to the mechanism of piezoelectric ceramics, its specific application in energy storage is analyzed.

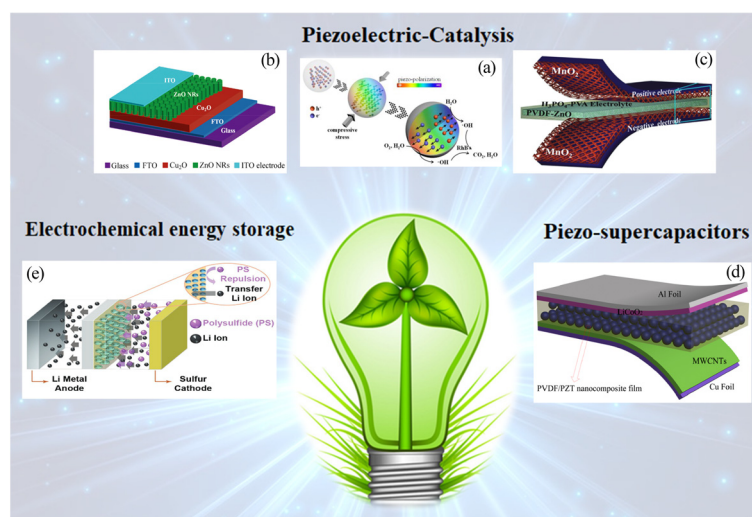


Figure 1. Piezoelectric ceramics are used in the energy field. (a) Proposed reaction mechanisms of piezo-catalysis. Reproduced with permission from [16]. Copyright 2017, Yawei Feng. (b) Schematic of the fabricated device. Reproduced with permission from [17]. Copyright 2014, Pei Lin (c) Schematic diagram of the fabricated SCSPC. Reproduced with permission from [18]. Copyright 2015, Ananthakumar Ramadoss. (d) Schematic structure image of SCPC with piezoelectric spacer Reproduced with permission from [19]. Copyright 2014, Yan Zhang. (e) The effect of the poled BTO toward polysulfide rejection. Reproduced with permission from [20]. Copyright 2016, Taeun Yim. (Reprinted with permission from [16–20]); Copyright 2017, *Nano Energy. Interfaces* 2017, 40, 481–486).

Herein, we focus on the latest advances in nano/micrometer-sized materials, such as BaTiO₃ nanowires (NWs), BaTiO₃ nano/micrometer-sized particles and ZnO nanorods (NRs). This review introduces the principles of piezoelectric electrocatalysis and the working principle of piezoelectric energy storage materials. The two processes of power generation and energy storage of traditional piezoelectric materials are integrated into one device, which realizes the process of the integration of power generation and energy storage.

2. Piezoelectric Catalysis for Hybrid Energy Devices

In piezoelectric catalytic hybrid devices, nano/micron materials, such as NWs, nanosheets and NRs, can generally convert mechanical stress into polarized charge, exhibiting effective bending compliance and flexibility. In addition, the separation efficiency of photoexcited charge carriers can be enhanced by the mutual coupling of photoexcited and piezoelectric nanomaterials in semiconductor photocatalysts. Nano/micrometer materials can be driven by micro-vibration energy, even muscle movement, resulting in the generating of piezoelectric potential. Researchers have recently discovered and studied the piezoelectric effect mediated by nano/micrometer-sized materials [2,21–23]. Several researchers report that piezoelectric catalysis was first used for degrading non-dye pollutants, demonstrating that this is an emerging and effective advanced oxidation technology for organic pollutant degradation and dichlorination [24]. At least three mechanisms, including the piezoelectric, piezo electrochemical and catalytic degradation processes, may have been engaged in piezo catalytic degradation. As is well known, there are three ways to employ the piezoelectric effect to accelerate the breakdown of organic contaminants. First, piezo catalysis, the direct application of the piezoelectric potential to the degradation of organic pollutants, is used. The piezoelectric potential of one- or two-dimensional piezoelectric materials is greater than that of particles. Consequently, the usage of nanoflowers NLs and NWs in piezo catalysis was widespread [16,25,26].

The catalytic action known as piezo catalysis is powered by the stress-induced electric-ity of piezoelectric crystallites [27,28]. In the absence of optical excitation and piezoelectric polarization, mechanical motion induces the piezo catalysis. Numerous electrochemical processes, including the breakdown of organic contaminants, the splitting of water and electrochemical polymerization, can be caused by piezoelectricity. It has proven to be a promising technology at the interface between energy and the environment. The mediated piezoelectric action by nano/micrometer-sized materials has been discovered and studied [29]. The piezoelectric process made the successful separation of photo-generated electron hole pairs possible, which can accelerate the breakdown of nanostructures.

Bao et al. [30] demonstrate that the charge carriers (rather than piezoelectric charges) inherent in piezoelectric crystals act as charge transfer agents, by modulating the concentration of charge carriers during catalysis. Piezoelectric BaTiO₃ NWs and nano/micrometer particles were synthesized, and their piezo catalytic activity was investigated. The piezoelectric activity of BaTiO₃ NWs can be attributed to the significant increase in pi-piezoelectric potential along the polar axis direction. On the other hand, hydrothermally synthesized nano/micron size tetragonal BaTiO₃ particles were used as piezoelectric catalysts, and low-frequency ultrasonic irradiation was chosen as vibrational energy to induce tetragonal BaTiO₃ deformation [24]. The 4-chlorophenol might be simultaneously dechlorinated and degraded by the piezoelectric potential from the deformation (Figure 2). The presence of lattice fringes across the individual grains in the TEM picture (Figure 2c) demonstrates that the grains are single crystalline. The piezoelectric process produced several active species, including h⁺, e⁻, •H, •OH, •O²⁻, ¹O₂ and H₂O₂. These findings demonstrate the effectiveness of piezo catalysis as a cutting-edge oxidation method for the degradation and dichlorination of organic contaminants. According to Lin et al. [31], the preferential deposition of Ag nanoparticles at the positive polar end of BaTiO₃ nanocubes/cubes through piezo electrochemical and photochemical processes can enable the free charge carriers to play a full role in hydroxyl radical generation, thus greatly enhancing piezoelectric catalytic degradation performance.

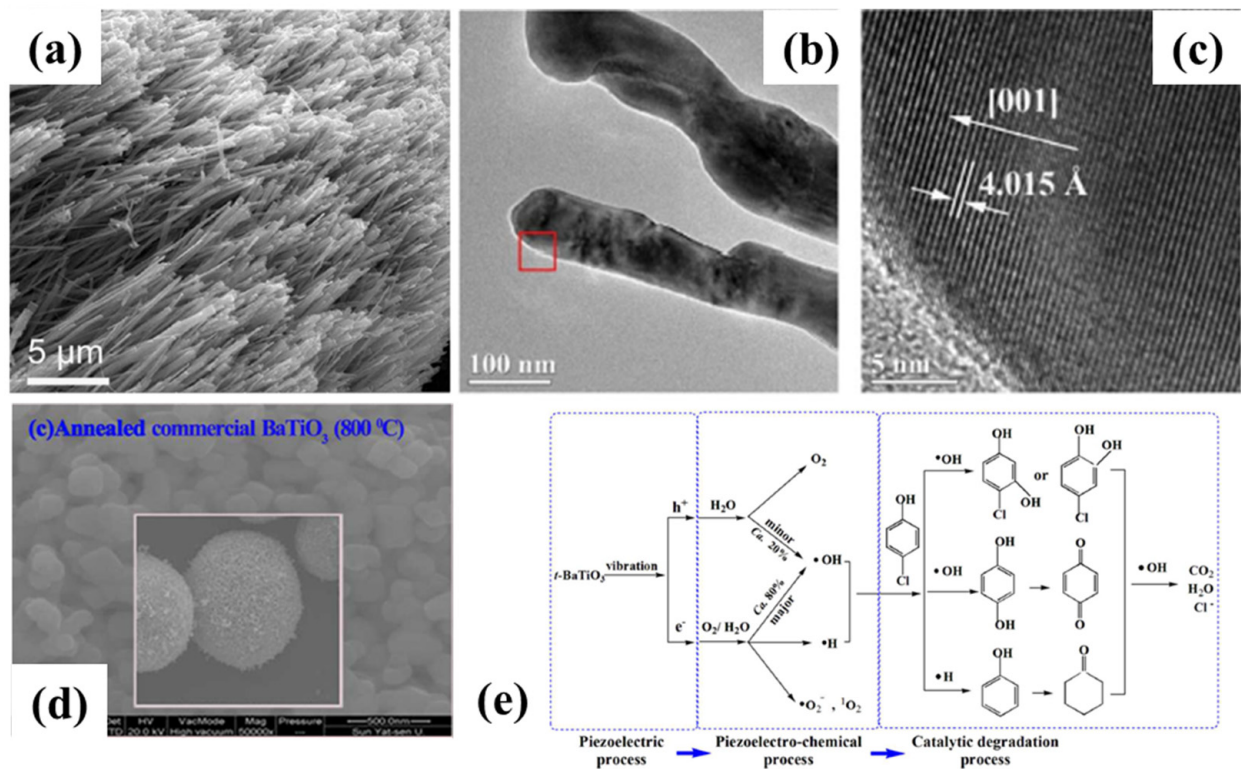


Figure 2. (a) Hydrothermal BaTiO₃ nanowires (BTO-1) in SEM pictures. (b,c) Images of hydrothermal BaTiO₃ nanowires, captured by TEM and HRTEM. Reproduced with permission from [30]. Copyright 2018, Jiang Wu. (d) SEM micrographs of annealed commercial BaTiO₃ at 800 °C. (e) Primary Routes for 4-CP Degradation in the t-BaTiO₃-Mediated Piezo-Catalysis Process. Reproduced with permission from [24]. Copyright 2017, Shenyu Lan. (reprinted with permission from [24], Copyright 2017, *Environ. Sci. Technol. Interfaces* **2017**, 51, 11, 6560–6569).

ZnO additionally offers the benefit of being environmentally benign, in addition to BaTiO₃. ZnO is a novel piezoelectric material, known for its affordable, environmentally benign and chemically stable properties. It was discovered that the effective piezoelectric coefficient was high [32]. The ZnO nanorods demonstrated significant vibration–catalytic activity, by using the linkage of the piezoelectric effect and the electrochemical process. Acid orange 7(AO₇) solution (5 mM) has a vibration catalytic decolorization ratio of as high as ~80%. The catalytic vibration process was achieved by creating electric charges triggered by piezoelectricity. Z. A. Ujjan et al. [33] showed a decrease in the optical band gap of ZnO, after the simultaneous doping of Cl^{−1} and S^{−2} in ZnO by a hydrothermal method, leading to an increase in the density of active sites and a decrease in the charge recombination rate of electron–hole pairs, which significantly improved the photocatalytic performance of ZnO for methylene blue (MB). However, the morphology of the nanorods remained essentially unchanged.

Moreover, there were some researches concerning all-oxide systems, such as ZnO, MnO₂ and Cu₂O/ZnO. By using the piezotronic effect, the photoresponse of an all-oxide Cu₂O/ZnO heterojunction was improved [17]. The band modification caused by interfacial piezoelectric polarization may be viewed in terms of this amplification, according to the Cu₂O/ZnO. Under illumination, the ZnO side’s positive piezopotential supplied an additional pushing force to separate the excitons more effectively (Figure 3).

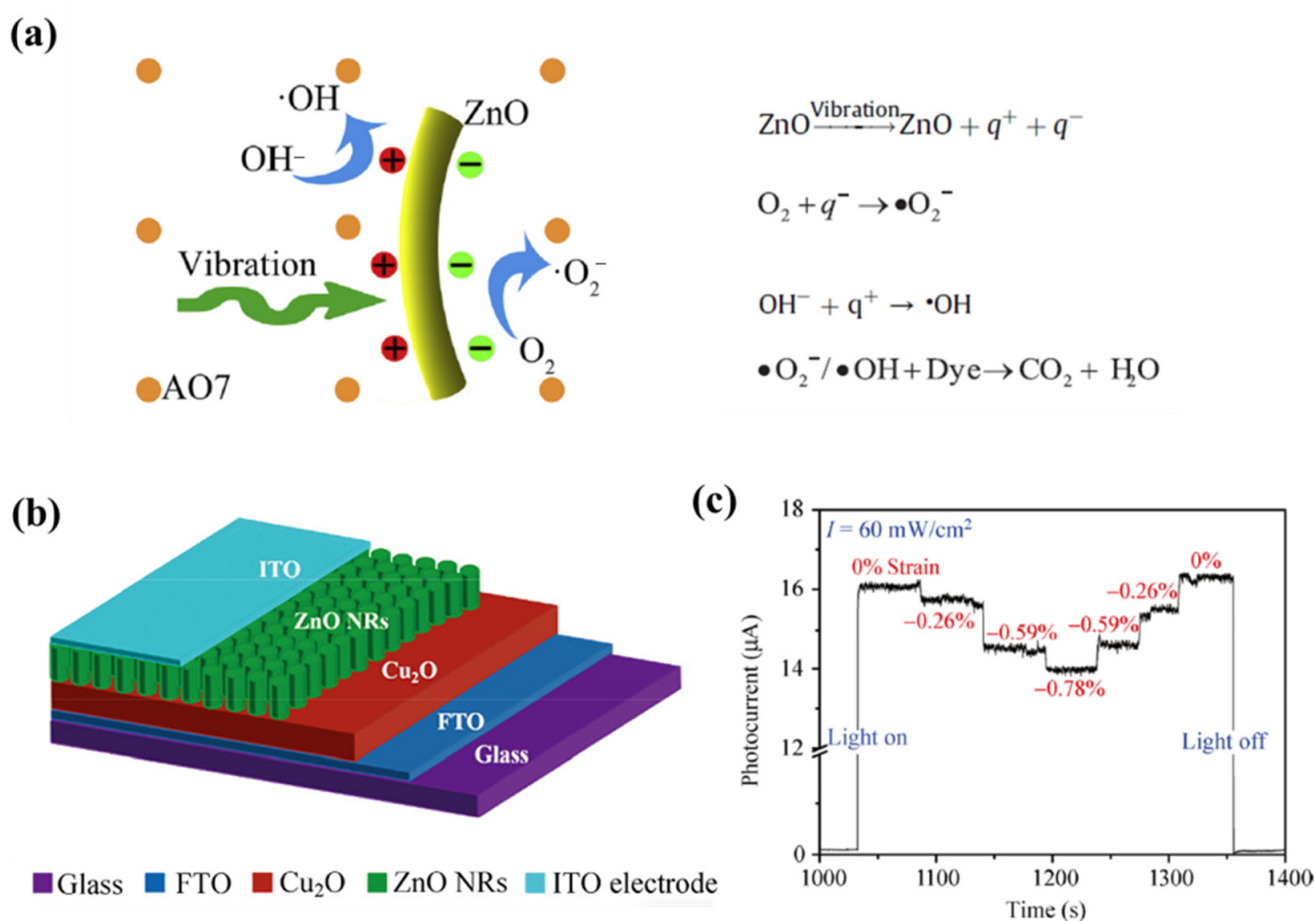


Figure 3. (a) The designed basic principle of the vibration–catalytic process; equations of the vibration–catalytic effect of ZnO nanorods. Reproduced with permission from [32]. Copyright 2018, Xiaoli Xu (b) Schematic of the control device Cu₂O/ZnO. (c) Reversibility test of the piezoelectric modulation with decreasing applied compressive strain. Reproduced with permission from [17]. Copyright 2014, Pei Lin (reprinted with permission from [17]; Copyright 2014, *Nano Res. Interfaces* **2014**, 7, 6, 860–868).

The Li and Bian group created lead zirconate titanate (PZT), a piezoelectric material with a spherical form [16]. There are free charges in piezoelectric materials, which may be generated by narrow band gap semiconductors or defect doping. The piezoelectric material generates an internal electric field to separate the free charges during the compression process. At the surface of the piezoelectric material, the free charge triggers a redox process that produces oxidatively active chemicals that break down dye molecules into carbon dioxide and water (Figure 4). More significant than the morphological structure of the material, PZT’s distinctive spherical form may create piezoelectric catalytic activity. Piezoelectric materials may be utilized to collect and contaminate discrete mechanical energy. It is crucial for piezoelectric catalyst development and piezoelectric catalysis applications. In Zhang et al. [34], the chemical reaction driving force for the catalytic reduction of CO₂ by piezoelectric particles is when Nb-doped PZT lead piezoelectric particles are subjected to polarization changes at a low Curie temperature ($T_c \sim 38^\circ\text{C}$) in an ultrasonic, vibrational environment.

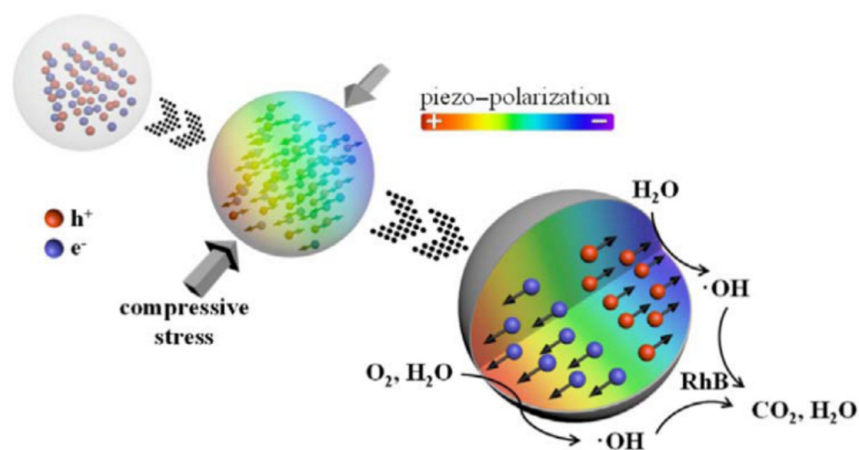


Figure 4. Proposed reaction mechanisms of piezo catalysis. Reproduced with permission from [16]. Copyright 2017, Yawei Feng. (reproduced with permission from [16]; Copyright 2017, *Nano Energy Interfaces* 2017, 40, 481–486).

The primary cause of the degradation and dichlorination was determined to be $\cdot\text{OH}$ radicals, produced by the electron reduction of O_2 and hole oxidation of H_2O . These inquiry findings demonstrate the effectiveness of piezo catalysis as a new and practical oxidation approach for environmental cleanup. Numerous intricate procedures, such as constructing heterojunction structures [35,36], doping [37] and decorating with noble metal particles [38], have been shown to increase the efficiency of light energy harvesting. The mainstream has recently been introduced to a more ambitious trend that aims to create a catalytic system without the need for light irradiation.

The Jyh-Ming Wu group [39] demonstrated the ultra-high degradation activity of monolayer and layer-less MoSe_2 nanoflowers to decompose rhodamine (RhB) dyes through the piezoelectric catalyst effect. By applying mechanical forces (e.g., ultrasonic vibrations) in the dark, the MoSe_2 nanofluid can successfully decompose 90% of the RhB dye within 30 s. This is the first work to demonstrate very efficient catalytic and redox processes using the piezoelectric catalyst effect of the MoSe_2 nanofluid.

3. Piezo Supercapacitors

As the name implies, a supercapacitor is a device that stores energy and functions similarly to a rechargeable battery because it can store electrical energy. The voltage is provided; its charge carrier can be kept inside. Since a direct current cannot flow inside a conventional capacitor, its essential components are two parallel plates separated by a dielectric. However, supercapacitors do not use dielectric materials. They have two identical leaves, separated by a very thin insulator and immersed in an electrolyte. Preference should be given to low loads to study the inherent electrochemical properties because the thickness of the electrodes expands with an increasing load, and the restricted ionic conductivity, combined with the voltage drop caused by the electronic conductivity, can create problems such as transfer beyond the thickness. Piezoelectric devices are one way to harvest mechanical energy to achieve the conversion of electric energy. Piezoelectric materials have been used in sensor application, semiconductor and supercapacitors, etc., [40].

MnO_2 is a novel, piezoelectric material as super capacity due to its low cost, pollution-free, rich resources and a good capacitor performance and safety process in preparations [41]. They investigated three asynchronous types of MnO_2 nanostructures, synthesized by a simple, hydrothermal process in the same system by changing the surfactant, the type of which determines the formation of MnO_2 nanostructures, namely NWs, nanoflowers (NFs) and NRs. A type of 40 μm diameter and 15 nm wide, single-crystal MnO_2 ultralong nanowire exists [42]. The materials demonstrated improved electrical conductivity, with a capacitance of 345 F/g at a current density of 1 A/g. They additionally had high-rate capability (54.7% at 10 A/g) and strong cycling stability (Figure 5).

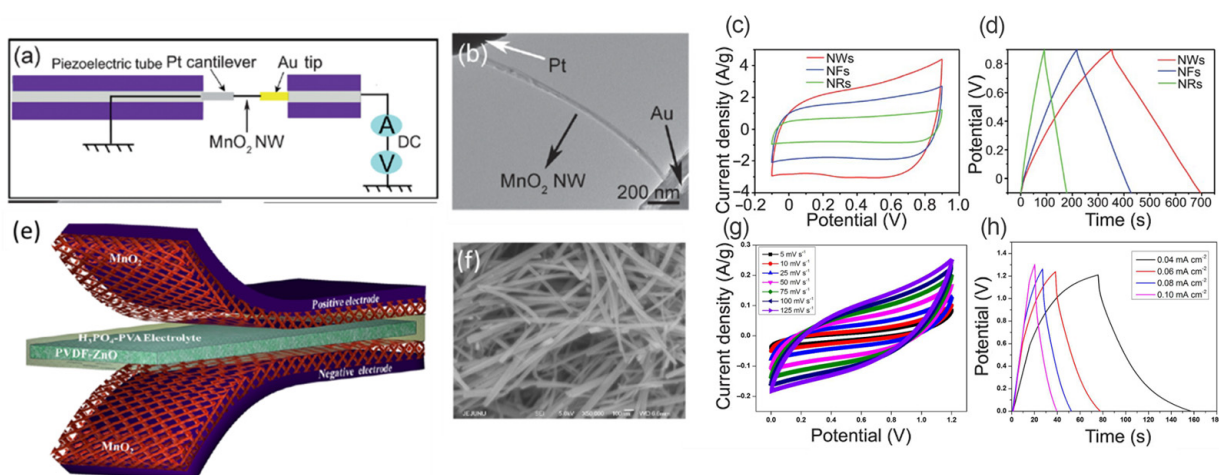


Figure 5. (a) Diagrams showing the electrical experimentation set up within an STM–TEM holder. (b) An individual MnO_2 NW was placed between a platinum cantilever and an Au tip in the boxed region, as seen in a TEM image. (c) CV curves using a 10 Mv/s scan rate. (d) Curves of charge–discharge, with a current density of 1 A/g. Reproduced with permission from [42]. Copyright 2012, Wenyao Li. (e) Schematic diagram of the fabricated SCPCs. (f) Picture of the FE–SEM nanostructure of MnO_2 . It demonstrates how nanowires are consistently sound. (g) SCPC cyclic voltammetry scans at various scan speeds. (h) SCPCs at various current densities, exhibiting galvanostatic charge/discharge curves. Reproduced with permission from [43]. Copyright 2015, Ananthakumar Ramadoss. (reprinted with permission from [18]; Copyright 2012, *J. Mater. Chem. A. Interfaces* 2012, 22, 30, 14864–14867).

Poly-vinylidene fluoride (PVDF) can be used as a wearable energy source and can convert irregular mechanical vibration into electricity [43]. There is enough energy for accumulating and storing electronic devices and systems to release the integration of energy harvesting and storage devices. Self-charging power cells (SCPCs), which convert and store energy, are typically constrained by slow charging and poor cyclability. Specific studies show that super capacity has a greater charging rate, better cyclability and higher power density [40,44]. The hybrid piezo supercapacitor integrates energy storage and harvesting into a single component. The piezo supercapacitor exhibits a 400 mW m^{-2} power density and a $49.67 \text{ mW h m}^{-2}$ energy density, while maintaining solid mechanical strength.

Recent reports describe piezoelectric polyvinylidene fluoride (PVDF) film sensors with CNT electrodes [45,46]. The energy from the piezoelectric materials was provided by low-frequency harmonic motion and used to charge the solution-processable supercapacitor, printed from a CNT dispersion. The transducer in a passive rectifying circuit was made of stiff piezo materials and rolled PVDF films.

4. Piezoelectric-Based Self-Charging Devices

Four types of interface circuits, synchronous energy harvesting (SEH) circuits, synchronous charge extraction (SCE) circuits, parallel synchronous switch harvesting on inductors (P-SSHI) courses and series synchronous switch harvesting on inductors (S-SSHI) circuits, have been thoroughly studied in piezoelectric energy harvesting over the past two decades. Many studies have looked at how to charge the electrical energy produced by PEH into a storage capacitor. Wu et al. [47] investigated this using the uncoupling premise of SEH circuits to capture the electrical energy from PEH into a storage capacitor. However, this analysis must be adjusted for PEH under moderate or vigorous coupling conditions. Wickenheiser et al. [48] examined the SEH circuits' ability to charge PEHs. It was nevertheless limited to PEHs having resonant vibrations. Bagheri et al. proposed an iterative numerical method and studied the transient charging behavior of cantilever beams with piezoelectric patches, using SHE [49] and SSHI circuits [50]. In particular, when

self-powered SSHI is implemented using electronic circuit breakers, a nonlinear treatment by self-powered SSHI circuits can significantly increase power-collecting efficiency during charging. Zhang et al. [51] centered on modelling and comparing these four circuit-charging processes. First, it was established that an ideal storage capacitor exists for SEH, P-SSHI or S-SSHI circuits to optimize the collected energy, varied by coupling conditions. The P-SSHI circuit is appropriate for weak coupling PEH energy charging. The SEH and S-SSHI circuits are more effective for moderate and robust coupling conditions than the P-SSHI and SCE circuits.

Energy harvesting and storage are often accomplished by two independent components in one electronic device and are two distinct electrochemical processes [52]. If the energy storage units, such as Li-ion batteries (LIBs) and SCs, can be integrated with energy storage components, the final electronics could be made seamlessly and with more functions. SCPCs collect electrical energy from mechanical energy through a piezoelectric polymer, PVDF diaphragm and store it in the battery electrode through a piezo electrochemical conversion process. SCPCs are a button-type battery, consisting of an anode and cathode. The anode is an anatase TiO_2 arranged in nanotubes on a titanium foil, the cathode being LiCoO_2 with a conductive agent, and the carbon/binder mixture material on the aluminum foil and diaphragm is polarized PVDF film [53]. The SCPCs realize energy harvesting and storage in one unit, which significantly enhances the total efficiency of that of separated devices under the same conditions. More importantly, these self-charging devices can harvest environmental energy continuously, which may make them an ideal power source for future electronics [54].

The first concept and device was developed by Wang et al. [21], which is based on a piezoelectric effect. Using a piezoelectric effect, mechanical energy is immediately transformed in this device into electrochemical energy, which is then stored in an LIB or SC. The ability of some solid materials to collect an electric charge in response to mechanical stress, known as piezoelectricity, makes them suited to harvesting fluctuating environmental, mechanical energy. The basic idea behind self-charging LIBs or SCs is to swap out conventional polymer separators for piezoelectric PVDF films that can convert mechanical energy into electrochemical energy and store it once the device has recovered from mechanical distortion. The self-charging LIB is initially in a discharge condition, where LiCoO_2 , graphite and LiPF_6 serve as the positive, negative and electrolyte (Figure 6). In response to external compressive stress on the battery, the polarized PVDF piezoelectric separator deforms compressively and generates a piezoelectric electric field in the thickness direction. In response, the lithium ions in the electrolyte redistribute and move to the cathode part to combat the piezoelectric field produced by the PVDF separators. Due to the disruption of the electrochemical equilibrium, some lithium ions from the LiCoO_2 cathode de-intercalate to form Li_xC_6 . A new equilibrium is reached after the migration of Li^+ balances the piezoelectric field. When the external compressive stress disappears, the piezoelectric field produced by PVDF separators then disappears. This disappeared piezoelectric field additionally produces the re-distribution of lithium ions, and a part of the lithium ions moves back to the LiCoO_2 side, whereas a small portion of lithium ions are left in the graphite side. As a result, a small quantity of mechanical energy is transformed and stored directly in these charging LIBs. By applying periodic, compressive stress to the self-charging LIBs, this self-charging process happens repeatedly to realize the full charging of the LIBs. With the exception of self-charging LIBs, this self-charging mechanism can be additionally applied to aqueous or organic super capacitors [55,56]. Although the design principles and architecture for piezoelectric-based SCPC is quite simple, it still faces some difficult problems to solve towards practical applications. The main questions and resolutions are as follows.

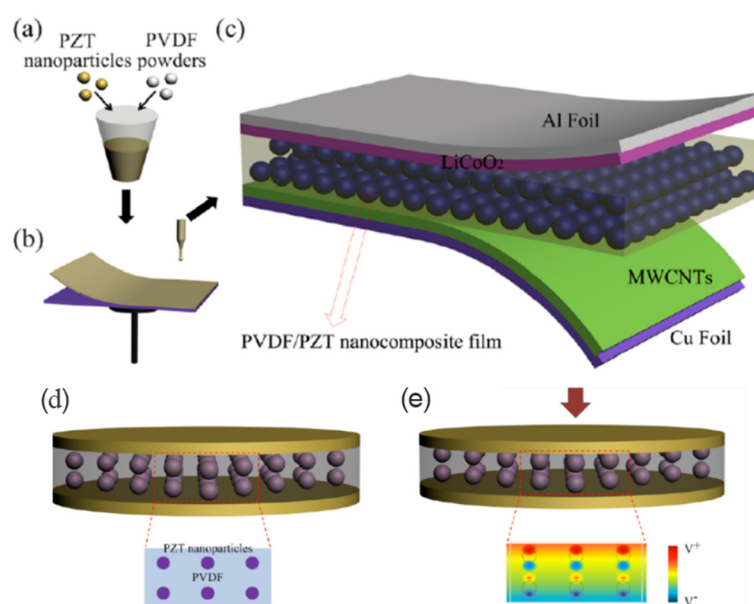


Figure 6. (a,b) PVDF–PZT nanocomposite film production process schematic pictures. (c) PVDF–PZT nanocomposite film in the schematic construction of an SCPC as the piezo separator for the charge storage component. (d) The cross-sectional view of six PZT nanoparticles scattered throughout the PVDF. (e) Piezo potential distribution in a schematic picture under external compressive stress. The dispersion of the PVDF–PZT nanocomposite film’s pseudopotential is depicted by its color code. Reproduced with permission from [19]. Copyright 2014, Yan Zhang. (reprinted with permission from [19]; Copyright 2014, *Nanotechnology. A. Interfaces* **2014**, *10*, 25, 105401).

4.1. Self-Charging Efficiency

One of the major difficulties for SCPC lies in its extremely low self-charging efficiency. Table 1 shows the materials, configuration and performance of piezoelectric materials-based SCPC. For instance, the open-circuit voltage of a typical LiCoO₂/PVDF/TiO₂ nanotube self-charging LIB only grew from 327 to 395 mV in 240 s under the compressive force of 45 N at a frequency of 2.3 Hz, which translates to 0.036 μAh. Other typical self-charging LIBs or SCs are in order of ~μAh as well, as shown in Table 1. This self-charging capability is much below the realistic requirements, and further work is needed for practical applications. This is because the self-charging device has a sluggish charging speed and must be subjected to mechanical force for a long time.

Table 1. Materials, configuration and performance of piezoelectric materials-based SCPC device.

Electrode	Piezoelectric Materials	Electrolyte	Self-Charging Capacity	Self-Charging Performance	Ref.
LiCoO ₂ (coating) TiO ₂ nanotube (electrochemical anodizing)	PVDF	LiPF ₆ /EC:DMC	0.036 μAh	327 to 395 mV in 240 s with 45 N at 2.3 Hz	[8]
MoSe ₂ nanosheets	NaNbO ₃ /PVDF	PVDF-co-HFP/TEABF ₄	18.93 F/cm ²	Up to 708 mV in 100 s with 30 N	[57]
CNT	P(VDF-TrFE)	PMMA/PC/LiClO ₄	95 μF/cm ²	Up to 70 mV with 50 N at 10 Hz	[58]
FCC	PVDF	PVA/H ₂ SO ₄	0.25 μAh	0~100 mV in 40 s with 2000 s without any external forces at 4.5 Hz	[59]

Table 1. Cont.

Electrode	Piezoelectric Materials	Electrolyte	Self-Charging Capacity	Self-Charging Performance	Ref.
LiCoO ₂ /MWCNTs	PVDF-PZT	LiPF ₆ /EC:DMC	~0.010 μAh	210 to 297.6 mV in 240 s with 10 N at 1.5 Hz	[19]
LiCoO ₂ /graphite	PVDF-ZnO	LiPF ₆ /EC:DMC	~0.173 μAh	160 to 300 mV in 240 s with 34 N at 1.8 Hz	[60]
NiCoOH-CuO@Cu RGO@Cu	Bio-piezoelectric separator	PVA-KOH	~0.424 μAh	130.1 to 281.3 mV in 80 s with finger imparting at 1.65 Hz	[61]
LiCoO ₂ /graphite	PVDF/ZnO	LiPF ₆ /EC:EMC	3.04 μAh	1335 at 1400 mV in 200 s with 282 mJ at 1 Hz	[9]
LiCoO ₂ /graphite	PVDF	LiPF ₆ /EC:DEC:DMC	0.118 μAh	105 to 220 mV in 300 s with 30 N at 1 Hz	[62]
LiCoO ₂ CuO	PVDF	LiPF ₆ /EC: DMC	0.0247 μAh	90 mV increment in 240 s with 18 N at 1 Hz	[63]
LiCoO ₂ graphene	PVDF	LiPF ₆ /EC: DMC	0.266 μAh	500 to 832 mV in 500 s with 34 N at 1 Hz	[64]
MnO ₂ nanowires	PVDF-ZnO	PVA/H ₃ PO ₄	/	110 mV increment in 300 s under palm impact	[18]

FCC: functionalized carbon cloth.

The low self-charging efficiency of the piezoelectric-based SCPC can be partly improved by adding suitable, inorganic piezoelectric materials with a high permittivity coefficient. For example, inorganic NaNbO₃ [57], PZT [19] or ZnO [9] materials were added to form high-efficiency piezoelectric electrolyte (Table 1). Pazhamalai et al. [57] used 2D MoSe₂ as an electrode and PVDF/NaNbO₃ as the piezopolymer electrolyte. Compared to the naked PVDF, the piezo output was significantly improved by the PVDF/NaNbO₃ nanofibrous mat. Peak to peak voltage for the NaNbO₃/PVDF was approximately 4 V. Kim et al. [9] included ZnO particles to create a piezoelectric β-form PVDF separator with a very porous structure. The electrochemical charge/discharge performance was significantly improved, compared to the less porous PVDF sheet. The PVDF–PZT nanocomposite film was compared with the pure PVDF film, and PZT could increase the piezoelectric potential. The charging capacity of the PVDF–PZT nanocomposite film-based SCPC was ~0.010 μAh in 240 s, which was higher than that of the pure PVDF film-based SCPC (~0.004 μAh), compared with the pure PVDF film-based SCPC [19].

Another important strategy to improve the self-charging efficiency is to build an integrated porous self-charging electrode, with an interpenetrated architecture. For example, Xue et al. [63] built an integrated CuO/PVDF nanocomposite piezoelectric anode operated by spin-coating PVDF onto a CuO nanoarray. They found that the efficiency of the integrated SCPC was higher than that of the non-integrated SCPC. The tight and extensive contact between the CuO nanoarray and PVDF led to the efficient utilization of the piezoelectric field in the internal piezoelectric process. Supercapacitors possess lower energy density, while showing significantly better charge/discharge speeds than those of LIBs. Furthermore, Parida et al. [58] used CNT electrodes to create a self-powered, electric, double-layer supercapacitor. This SCPC device has a fast-charging capability, due to the rapid adsorption and desorption of ions at the surface of CNT electrodes; 90% of the voltage increase (approximately 60 mV) was completed in less than 10 s. The piezoelectric porous P(VDF-TrFE) foam used in this design contains a lot of pores, which helps with ion transport and electrolyte absorption.

4.2. Flexibility

The materials, designs and production techniques for wearable technology have advanced significantly during the last ten years. One of the most significant problems

hindering the success of wearable gadgets is the development of flexible LIBs or SCs. Until now, great achievements were obtained in this field [65]. In order to obtain a flexible electrode, active materials of LIBs or SCs have usually been deposited on conformal substrates (paper, plastic, cotton, CNTs or graphene films, etc.) to a certain flexibility. If the flexibility and self-charging ability can be integrated into one device, the final LIBs or SCs can be widely used in future electronics. Currently, the conventional electrodes of self-charging devices are usually based on a slurry coating process. Repeated stresses easily result in micro-cracks of the electrodes and a detachment of active materials from metal substrates. On the other hand, most mechanical energy is adsorbed by rigid packing materials when not transformed into electrochemical energy. This rigid design and architecture significantly lower the conversion efficiency. More importantly, conventional, rigid, coin cell design is not suitable for the growing demand of wearable devices. In order to fully utilize environmental mechanical energy, we can combine relevant results from the research of flexible piezoelectric materials. For example, Luo et al. [66] created a flexible, BaTiO₃/polydimethyl siloxane (PDMS) thin layer that can provide solid and constant electrical outputs when subjected to repeated, mechanical pounding. An energy-storage capacitor could light a red LED, and the flexible composite film could produce a maximum output voltage of 7.43 V. Lin et al. [67] additionally created a stretchable piezoelectric membrane, using a mix of PDMS substrate and BaTiO₃ nanotubes. This promising and adaptable technology might be used to develop flexible SCPC devices.

5. Piezoelectric Materials in Electrochemical Energy Storage

Driven by increasingly stringent environmental regulations worldwide, auto manufacturers are all striving to expand their offer of electric vehicles, including hybrid (HEV) and battery electric vehicles (BEVs), in a fairly tight time scale. LIBs have found more and more extensive applications because of their excellent performance. In the current era, a higher energy density, rate performance and low temperature performance are still ever-growing requirements for LIBs to power EVs. Due to their unique properties, various piezoelectric materials open new doors for the improvement of LIBs materials. The application of piezoelectric materials in LIB materials has three aspects: (a) the improvement of electronic/ionic conductivity, thereby leading to better rate and low temperature performance; (b) buffer volume expansion/contraction during charging/discharging processes for silicon anodes; (c) acting as a coating layer to improve the cathode's cycling performance; and (d) lower interface resistance in solid state LIBs.

Silicon (Si) has a much larger energy density than conventional graphite anode, and it is highly anticipated in high-energy density LIBs. Unfortunately, the most significant barrier to commercializing silicon anode is the silicon's significant volume shift when lithium is introduced. Strategies have been devised to control the volume variation during charge/discharge cycles to increase the cycle performance of silicon anodes. These include reducing the silicon particle size to nano-size, designing novel silicon nano-architecture, fabricating Si/C composite materials, etc., [68,69].

Lee et al. [70] introduced BaTiO₃ piezoelectric materials to the Si/CNT anode materials. During charging/discharging processes, stress is induced by silicon-polarized BaTiO₃ materials. This local piezoelectric potential may affect the mobility of Li-ions, which enhances the electrochemical performance of the Si/CNT/BaTiO₃ nanocomposite anode. As shown in Figure 7c,d, piezoelectric BaTiO₃ additives significantly improve the cycle performance of a silicon anode (Figure 7). According to the directions of the applied piezoelectric potentials, density functional calculations show that diffusion may be increased or decreased by using piezoelectric potentials. When the piezoelectric field is directed down the diffusion route, the obstacles to diffusion weaken with increasing field intensity. The primary mechanism controlling the diffusivity of Li-ions in Si surfaces is diffusion from the surface to the subsurface. Due to the presence of the piezoelectric field and the ability to boost the diffusivity by $\sim 10^5$ – 10^6 times with an applied piezoelectric field of 5 V/nm for surface diffusion, the diffusion barriers are significantly reduced [71].

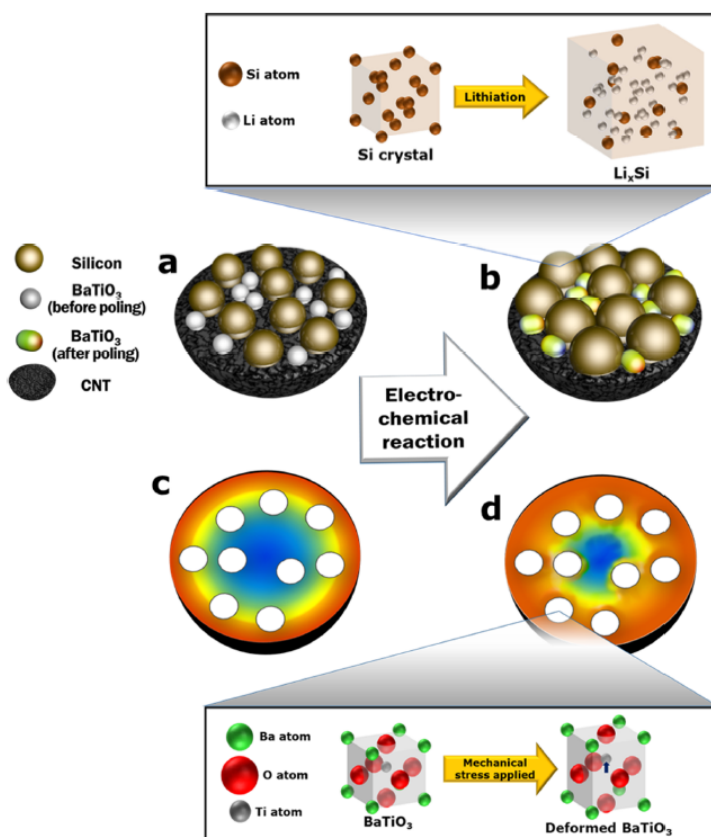


Figure 7. Schematic diagrams of how the Si/CNT/BTO nanocomposite anode's microstructure changed during lithiation. (a) Particles of Si and BTO are evenly scattered throughout and firmly adhered to the thick CNT. (b) Lithiation of the Si nanoparticles causes a significant volume increase, pressurizing and poling the BTO nanoparticles to produce a piezoelectric potential. (c) Without piezoelectric poling, the high current density (shown in red) is only noticeable at the particle surfaces. (d) The mobility of the Li-ions is improved during the following charging and discharging operations by a permanent and local piezoelectric potential, which leads to a high current density. The images in the box show the microstructural alterations in Si (expansion brought on by lithiation) and BTO₃ (piezoelectric poling brought on by Si expansion). Reproduced with permission from [70]. Copyright 2016, Byoung-Sun Lee. (reprinted with permission from [70]; Copyright 2016, *ACS Nano. Interfaces* 2016, 10, 2, 2617–2627).

One of the newest energy storage technologies is all-solid-state lithium batteries with solid electrolytes. Solid-state LIBs possess a wider potential operating window, inherent safety and higher density and could be used in long-distance electric vehicles. Lithium-oxynitride phosphate glass (Li_{3.2}PO_{3.8}N_{0.2}) has an upper potential limit of up to 5.5 V (vs. Li/Li⁺), which can act as a promising solid electrolyte. Yada et al. [72] built a 5 V-class Li/LiPON/LiCr_{0.05}Ni_{0.45}Mn_{1.5}O_{4-δ} all-solid-state LIB. Although the enormous charge transfer resistance at the Li/LiPON/LNM interface significantly reduced its electrochemical performance, the resulting Li/LiPON/LNM battery did not exhibit any overt charge/discharge processes at any potentials between 3.0 and 5.3 V. It is intriguing to note that the charge transfer resistance of the LiPON/LNM interface (R_{LiPON/LNM}) is more than 107 Ω cm² at 4.7 V, which is significantly higher than the 4 V-class Li/LiPON/LiCoO₂ resistance. According to one theory, the significant interface resistance was brought on by the enormous electric field (ELiPON/LNM) at the interface between the two materials (LNM-LiPON), which was thought to be the result of their significant electric potential difference. To lower the ELiPON/LNM value, the spin-coating of dielectric BaTiO₃ was conducted on the LiPON/LNM interfaces. The battery with the 100 nm BaTiO₃ modification retained 84% of its discharge capacity at 0.25 °C, whereas the unmodified battery displayed

only 45 mAh/g at the same rate. Figure 8 shows the mechanism of the BaTiO₃-modified interface. As shown in Figure 8, the large electric potential difference ($\Phi_{\text{LNM}} - \Phi_{\text{LiPON}}$) acts as a driving force to extract many lithium ions from the LiPON layer, which results in a Li⁺ deficient layer to block the Li⁺ transport. After the BaTiO₃ modification, Li⁺ originally located behind the BaTiO₃ layers was re-arranged due to the electric dipoles to maintain local charge neutralities and finally created a “Li⁺” pathway for charge-transfer reactions [20].

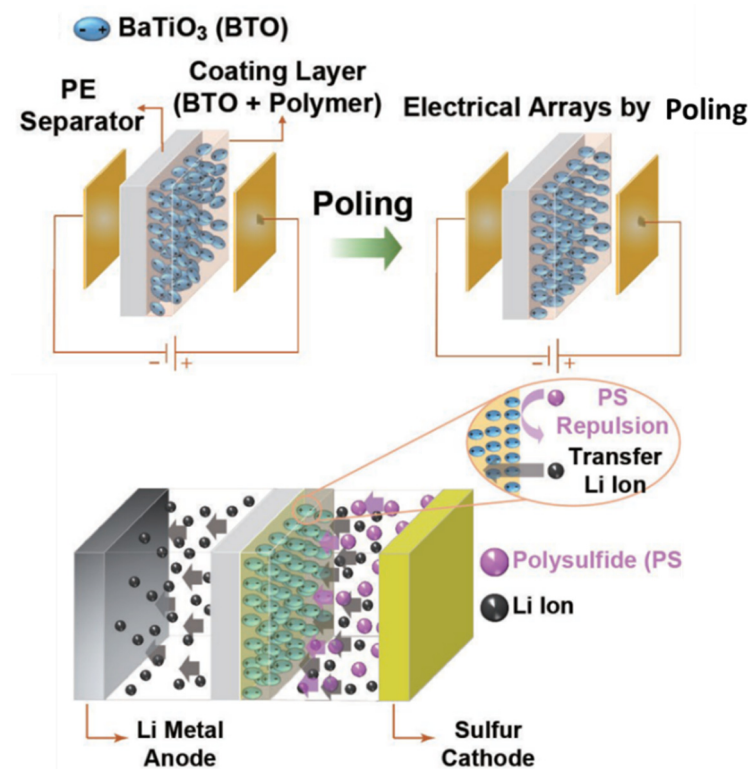


Figure 8. Diagrammatic representation of the poling of the PE separator coated with BTO and the impact of the poling on polysulfide rejection. Reproduced with permission from [20]. Copyright 2016, Taeun Yim. (reprinted with permission from [20]; Copyright 2016, *Adv. Funct. Mater. Interfaces* **2016**, *26*, 43, 7817–7823).

As a new battery system, Li-S batteries have an ultra-high energy density (theoretical value, 2600 Wh/Kg), which is 5 times higher than that of commercial LIBs. Unfortunately, a quick capacity decline mainly brought on by the shuttle effect of polysulfide has prevented its practical deployment. This problem is solved by including the spontaneously polarized BaTiO₃ nanoparticles in the composite sulfur cathodes. Because of the spontaneous polarization's internal electric field, the dissoluble heteropolar polysulfides would be absorbed in the vicinity of the polar BaTiO₃ nanoparticles [73]. With the addition of BaTiO₃, the composite sulfur cathode shows a reversible discharge capacity of 835 mAh/g after 100 cycles. A C/S composite cathode without the BaTiO₃ additive has only a reversible capacity of 407 mAh/g after 100 cycles. In order to suppress the shuttle effect of polysulfide, Yim et al. [20] coated poled BaTiO₃ nanoparticles on PE separators, which have an electrostatic repulsion barrier that effectively prevents polysulfide from flowing through the separator, leading to greatly increased cyclability. With this BaTiO₃-coated separator, the Li-S battery started at 1122.1 mAh/g and ended at 929.5 mAh/g after 50 cycles, which corresponds to 82.8% capacity retention. In contrast, the Li-S battery with an uncoated separator only delivers 59.4% capacity retention.

An efficient way to increase the cycle stability and rate performance for traditional cathode materials at higher rates is to cover them with an insulating oxide. The side reactions at the cathode/electrolyte interface can be suppressed by oxide surface coating [74]. Ferroelectric materials have a permittivity of a few thousand, which is far higher than

conventional oxide coatings such as Al_2O_3 , ZrO_2 , MgO , etc. This extremely high permittivity can result in interfacial polarization between the ferroelectric layer and the cathode surface. Lithium-ion transport kinetics may be affected by such an interfacial impact. Teranishi et al. [73] coated BaTiO_3 on the surface of LiCoO_2 cathode materials by a simple sol–gel synthesis. The high-rate capacities for the BaTiO_3 -coated LiCoO_2 were significantly higher than those for the bare LiCoO_2 materials. The coated BaTiO_3 ferroelectricity would cause an improvement in the high-rate performance [75]. Dielectric LiNbO_3 was additionally used to decorate the LiCoO_2 cathode. It was found that the crystalline single LiNbO_3 introduced dielectric polarization architecture that accelerated the Li transfer at the LiNbO_3 -active material–electrolyte triple-phase junctions. The highest discharge capacity of the LiNbO_3 -decorated LiCoO_2 was 78 mAh/g at a 20 °C rate, which is 2.6 times higher than that of bare LiCoO_2 at the same rate [76]. This is primarily due to the electric double-layer formed at the interface between the active material and the electrolyte during the Li solvation and desolvation process, which results in a Li-deficient layer with a high resistance to Li transfer. Similarly to the function of BaTiO_3 in solid-state LIBs, as stated before, LiNbO_3 additionally attracts the positively charged Li^+ to the Li-deficient layer, thus resulting in the increase of the lithium-ion concentration at the triple-phase boundary [77]. Co oxidation occurs when the LiCoO_2 modified by BaTiO_3 is charged, and this is evidence of the increased polarization brought on by the higher permittivity of $\text{BaTiO}_{3.6}$.

6. Conclusions

This review aims to provide insight into the importance of piezoelectric materials in different fields. We reviewed the intrinsic piezoelectric properties of other materials and discussed piezoelectric catalysis for hybrid energy devices, piezo-supercapacitors, piezoelectric-based self-charging devices and piezoelectric materials in electrochemical energy storage. This paper reviewed the recent advances in piezoelectric materials and their applications in different fields, where using these materials has significantly improved the frequency and energy characteristics of the piezoelectric devices developed on their basis. In the future, piezoelectric generators will power many electronic devices, and these advanced materials and transducers will be widely used to create devices for energy harvesting using infrastructure objects and vehicles, wearable flexibility, physical medicine, and the detection of human physiological functions. Despite their fascinating capabilities, current piezoelectric materials still face significant challenges that must be overcome. This review will provide reference value and give some necessary knowledge for applying advanced piezoelectric materials in various fields.

7. Patents

This section is not mandatory, however may be added if there are patents resulting from the work reported in this manuscript.

Author Contributions: Validation, J.L. and F.H.; investigation, S.W. and X.G.; resources, S.W.; data curation, S.W. and L.W.; writing—original draft preparation, S.W. and L.W.; writing—review and editing, X.H.; visualization, S.W. and L.W.; supervision, J.L. and F.H.; project administration, S.W.; funding acquisition, S.W. All authors have read and agreed to the published version of the manuscript.

Funding: This research was funded by the Scientific Research Program of Tianjin Municipal Education Commission, grant number 2019KJ137.

Data Availability Statement: Not applicable.

Acknowledgments: Thank you to the Scientific Research Program of Tianjin Municipal Education Commission (2019KJ137) for the support.

Conflicts of Interest: The authors declare no conflict of interest.

References

1. Chiang, C.L.; Tseng, S.M.; Chen, C.T.; Hsu, C.P.; Shu, C.F. Influence of molecular dipoles on the photoluminescence and electroluminescence of dipolar spirobifluorenes. *Adv. Funct. Mater.* **2008**, *18*, 248–257. [[CrossRef](#)]
2. Hu, Y.F.; Wang, Z.L. Recent progress in piezoelectric nanogenerators as a sustainable power source in self-powered systems and active sensors. *Nano Energy* **2015**, *14*, 3–14. [[CrossRef](#)]
3. Wankhade, S.H.; Tiwari, S.; Gaur, A.; Maiti, P. PVDF-PZT nanohybrid based nanogenerator for energy harvesting applications. *Energy Rep.* **2020**, *6*, 358–364. [[CrossRef](#)]
4. Gheibi, A.; Latifi, M.; Merati, A.A.; Bagherzadeh, R. Piezoelectric electrospun nanofibrous materials for self-powering wearable electronic textiles applications. *J. Polym. Res.* **2014**, *21*, 469. [[CrossRef](#)]
5. Park, T.; Kim, B.; Kim, Y.; Kim, E. Highly conductive PEDOT electrodes for harvesting dynamic energy through piezoelectric conversion. *J. Mater. Chem. A* **2014**, *2*, 5462–5469. [[CrossRef](#)]
6. Bae, S.H.; Kahya, O.; Sharma, B.K.; Kwon, J.; Cho, H.J.; Ozyilmaz, B.; Ahn, J.H. Graphene-P(VDF-TrFE) Multilayer Film for Flexible Applications. *ACS Nano* **2013**, *7*, 3130–3138. [[CrossRef](#)] [[PubMed](#)]
7. Wen, X.N.; Yang, W.Q.; Jing, Q.S.; Wang, Z.L. Harvesting Broadband Kinetic Impact Energy from Mechanical Triggering/Vibration and Water Waves. *ACS Nano* **2014**, *8*, 7405–7412. [[CrossRef](#)] [[PubMed](#)]
8. Xue, X.Y.; Wang, S.H.; Guo, W.X.; Zhang, Y.; Wang, Z.L. Hybridizing Energy Conversion and Storage in a Mechanical-to-Electrochemical Process for Self-Charging Power Cell. *Nano Lett.* **2012**, *12*, 5048–5054. [[CrossRef](#)]
9. Kim, Y.S.; Xie, Y.N.; Wen, X.N.; Wang, S.H.; Kim, S.J.; Song, H.K.; Wang, Z.L. Highly porous piezoelectric PVDF membrane as effective lithium ion transfer channels for enhanced self-charging power cell. *Nano Energy* **2015**, *14*, 77–86. [[CrossRef](#)]
10. Platt, S.R.; Farritor, S.; Garvin, K.; Haider, H. The use of piezoelectric ceramics for electric power generation within orthopedic implants. *IEEE-Asme Trans. Mechatron.* **2005**, *10*, 455–461. [[CrossRef](#)]
11. Qi, Y.; Kim, J.; Nguyen, T.D.; Lisko, B.; Purohit, P.K.; McAlpine, M.C. Enhanced Piezoelectricity and Stretchability in Energy Harvesting Devices Fabricated from Buckled PZT Ribbons. *Nano Lett.* **2011**, *11*, 1331–1336. [[CrossRef](#)] [[PubMed](#)]
12. Siddiqui, S.; Kim, D.I.; Duy, L.T.; Nguyen, M.T.; Muhammad, S.; Yoon, W.S.; Lee, N.E. High-performance flexible lead-free nanocomposite piezoelectric nanogenerator for biomechanical energy harvesting and storage. *Nano Energy* **2015**, *15*, 177–185. [[CrossRef](#)]
13. Cao, Y.S.; Zhang, F.; Sha, A.M.; Liu, Z.Z.; Li, J.R.; Hao, Y. Energy harvesting performance of a full-pressure piezoelectric transducer applied in pavement structures. *Energy Build.* **2022**, *266*, 112143. [[CrossRef](#)]
14. Wang, Z.L. Triboelectric Nanogenerators as New Energy Technology for Self-Powered Systems and as Active Mechanical and Chemical Sensors. *ACS Nano* **2013**, *7*, 9533–9557. [[CrossRef](#)] [[PubMed](#)]
15. Choi, J.W.; Aurbach, D. Promise and reality of post-lithium-ion batteries with high energy densities. *Nat. Rev. Mater.* **2016**, *1*, 16013. [[CrossRef](#)]
16. Feng, Y.W.; Ling, L.L.; Wang, Y.X.; Xu, Z.M.; Cao, F.L.; Li, H.X.; Bian, Z.F. Engineering spherical lead zirconate titanate to explore the essence of piezo-catalysis. *Nano Energy* **2017**, *40*, 481–486. [[CrossRef](#)]
17. Lin, P.; Chen, X.; Yan, X.Q.; Zhang, Z.; Yuan, H.G.; Li, P.F.; Zhao, Y.G.; Zhang, Y. Enhanced photoresponse of Cu₂O/ZnO heterojunction with piezo-modulated interface engineering. *Nano Res.* **2014**, *7*, 860–868. [[CrossRef](#)]
18. Ramadoss, A.; Saravanakumar, B.; Lee, S.W.; Kim, Y.S.; Kim, S.J.; Wang, Z.L. Piezoelectric-Driven Self-Charging Supercapacitor Power Cell. *ACS Nano* **2015**, *9*, 4337–4345. [[CrossRef](#)]
19. Zhang, Y.; Zhang, Y.J.; Xue, X.Y.; Cui, C.X.; He, B.; Nie, Y.X.; Deng, P.; Wang, Z.L. PVDF-PZT nanocomposite film based self-charging power cell. *Nanotechnology* **2014**, *25*, 105401. [[CrossRef](#)]
20. Yim, T.; Han, S.H.; Park, N.H.; Park, M.S.; Lee, J.H.; Shin, J.; Choi, J.W.; Jung, Y.; Jo, Y.N.; Yu, J.S.; et al. Effective Polysulfide Rejection by Dipole-Aligned BaTiO₃ Coated Separator in Lithium-Sulfur Batteries. *Adv. Funct. Mater.* **2016**, *26*, 7817–7823. [[CrossRef](#)]
21. Wang, X.D. Piezoelectric nanogenerators-Harvesting ambient mechanical energy at the nanometer scale. *Nano Energy* **2012**, *1*, 13–24. [[CrossRef](#)]
22. Zhang, P.C.; Chen, L.; Xu, T.L.; Liu, H.L.; Liu, X.L.; Meng, J.X.; Yang, G.; Jiang, L.; Wang, S.T. Programmable Fractal Nanostructured Interfaces for Specific Recognition and Electrochemical Release of Cancer Cells. *Adv. Mater.* **2013**, *25*, 3566–3570. [[CrossRef](#)] [[PubMed](#)]
23. Wang, H.Y.; Qian, F.; Wang, G.M.; Jiao, Y.Q.; He, Z.; Li, Y. Self-Biased Solar-Microbial Device for Sustainable Hydrogen Generation. *ACS Nano* **2013**, *7*, 8728–8735. [[CrossRef](#)] [[PubMed](#)]
24. Lan, S.Y.; Feng, J.X.; Xiong, Y.; Tian, S.H.; Liu, S.W.; Kong, L.J. Performance and Mechanism of Piezo-Catalytic Degradation of 4-Chlorophenol: Finding of Effective Piezo-Dechlorination. *Environ. Sci. Technol.* **2017**, *51*, 6560–6569. [[CrossRef](#)] [[PubMed](#)]
25. Hong, K.S.; Xu, H.F.; Konishi, H.; Li, X.C. Direct Water Splitting Through Vibrating Piezoelectric Microfibers in Water. *J. Phys. Chem. Lett.* **2010**, *1*, 997–1002. [[CrossRef](#)]
26. Hong, K.S.; Xu, H.F.; Konishi, H.; Li, X.C. Piezoelectrochemical Effect: A New Mechanism for Azo Dye Decolorization in Aqueous Solution through Vibrating Piezoelectric Microfibers. *J. Phys. Chem. C* **2012**, *116*, 13045–13051. [[CrossRef](#)]
27. Anton, S.R.; Sodano, H.A. A review of power harvesting using piezoelectric materials (2003–2006). *Smart Mater. Struct.* **2007**, *16*, R1–R21. [[CrossRef](#)]

28. Wang, X.D.; Song, J.H.; Liu, J.; Wang, Z.L. Direct-current nanogenerator driven by ultrasonic waves. *Science* **2007**, *316*, 102–105. [[CrossRef](#)]
29. Wang, Z.L.; Song, J.H. Piezoelectric nanogenerators based on zinc oxide nanowire arrays. *Science* **2006**, *312*, 242–246. [[CrossRef](#)]
30. Wu, J.; Qin, N.; Bao, D.H. Effective enhancement of piezocatalytic activity of BaTiO₃ nanowires under ultrasonic vibration. *Nano Energy* **2018**, *45*, 44–51. [[CrossRef](#)]
31. Lin, E.Z.; Kang, Z.H.; Wu, J.; Huang, R.; Qin, N.; Bao, D.H. BaTiO₃ nanocubes/cuboids with selectively deposited Ag nanoparticles: Efficient piezocatalytic degradation and mechanism. *Appl. Catal. B-Environ.* **2021**, *285*, 119823. [[CrossRef](#)]
32. Xu, X.L.; Jia, Y.M.; Xiao, L.B.; Wu, Z. Strong vibration-catalysis of ZnO nanorods for dye wastewater decolorization via piezo-electro-chemical coupling. *Chemosphere* **2018**, *193*, 1143–1148. [[CrossRef](#)] [[PubMed](#)]
33. Ujjan, Z.A.; Bhatti, M.A.; Shah, A.A.; Tahira, A.; Shaikh, N.M.; Kumar, S.; Mugheri, A.Q.; Medany, S.S.; Nafady, A.; Alnjiman, F.; et al. Simultaneous doping of sulfur and chloride ions into ZnO nanorods for improved photocatalytic properties towards degradation of methylene blue. *Ceram. Int.* **2022**, *48*, 5535–5545. [[CrossRef](#)]
34. Zhang, Y.; Phuon, P.T.T.; Duy, N.P.H.; Roake, E.; Khanbareh, H.; Hopkins, M.; Zhou, X.F.; Zhang, D.; Zhou, K.C.; Bowen, C. Polarisation tuneable piezo-catalytic activity of Nb-doped PZT with low Curie temperature for efficient CO₂ reduction and H₂ generation. *Nanoscale Adv.* **2021**, *3*, 1362–1374. [[CrossRef](#)]
35. Kohtani, S.; Hiro, J.; Yamamoto, N.; Kudo, A.; Tokumura, K.; Nakagaki, R. Adsorptive and photocatalytic properties of Ag-loaded BiVO₄ on the degradation of 4-n-alkylphenols under visible light irradiation. *Catal. Commun.* **2005**, *6*, 185–189. [[CrossRef](#)]
36. Wu, J.M.; Kao, W.T. Heterojunction Nanowires of Ag_xZn_{1-x}O-ZnO Photocatalytic and Antibacterial Activities under Visible-Light and Dark Conditions. *J. Phys. Chem. C* **2015**, *119*, 1433–1441. [[CrossRef](#)]
37. Wu, J.M.; Hsu, G.K.; Yeh, H.H.; Lin, H.C. Metallic Zinc Nanowires Effect in High-Performance Photoresponsive and Photocatalytic Properties of Composite Zinc Stannate Nanowires. *J. Electrochem. Soc.* **2012**, *159*, H497–H501. [[CrossRef](#)]
38. Wu, J.M.; Tsay, L.Y. ZnO quantum dots-decorated ZnO nanowires for the enhancement of antibacterial and photocatalytic performances. *Nanotechnology* **2015**, *26*, 395704. [[CrossRef](#)]
39. Wu, M.H.; Lee, J.T.; Chung, Y.J.; Srinivas, M.; Wu, J.M. Ultrahigh efficient degradation activity of single- and few-layered MoSe₂ nanoflowers in dark by piezo-catalyst effect. *Nano Energy* **2017**, *40*, 369–375. [[CrossRef](#)]
40. Jin, H.Y.; Peng, Z.H.; Tang, W.M.; Chan, H.L.W. Controllable functionalized carbon fabric for high-performance all-carbon-based supercapacitors. *Rsc Adv.* **2014**, *4*, 33022–33028. [[CrossRef](#)]
41. Dai, Y.; Wang, K.; Xie, J.Y. From spinel Mn₃O₄ to layered nanoarchitectures using electrochemical cycling and the distinctive pseudocapacitive behavior. *Appl. Phys. Lett.* **2007**, *90*, 104102. [[CrossRef](#)]
42. Li, W.Y.; Liu, Q.; Sun, Y.G.; Sun, J.Q.; Zou, R.J.; Li, G.; Hu, X.H.; Song, G.S.; Ma, G.X.; Yang, J.M.; et al. MnO₂ ultralong nanowires with better electrical conductivity and enhanced supercapacitor performances. *J. Mater. Chem.* **2012**, *22*, 14864–14867. [[CrossRef](#)]
43. Tuukkanen, S.; Julin, T.; Rantanen, V.; Zakrzewski, M.; Moilanen, P.; Lilja, K.E.; Rajala, S. Solution-processible electrode materials for a heat-sensitive piezoelectric thin-film sensor. *Synthetic Metals* **2012**, *162*, 1987–1995. [[CrossRef](#)]
44. Wen, L.; Chen, J.; Liang, J.; Li, F.; Cheng, H.M. Flexible batteries ahead. *Natl. Sci. Rev.* **2017**, *4*, 20–23. [[CrossRef](#)]
45. Tuukkanen, S.; Julin, T.; Rantanen, V.; Zakrzewski, M.; Moilanen, P.; Lupo, D. Low-Temperature Solution Processable Electrodes for Piezoelectric Sensors Applications. *Jpn. J. Appl. Phys.* **2013**, *52*, 05da06. [[CrossRef](#)]
46. Lan, L.Y.; Xiong, J.Q.; Gao, D.C.; Li, Y.; Chen, J.; Lv, J.; Ping, J.F.; Ying, Y.B.; Lee, P.S. Breathable Nanogenerators for an On-Plant Self-Powered Sustainable Agriculture System. *Acs Nano* **2021**, *15*, 5307–5315. [[CrossRef](#)]
47. Wu, W.J.; Wickenheiser, A.M.; Reissman, T.; Garcia, E. Modeling and experimental verification of synchronized discharging techniques for boosting power harvesting from piezoelectric transducers. *Smart Mater. Struct.* **2009**, *18*, 55012. [[CrossRef](#)]
48. Wickenheiser, A.M.; Reissman, T.; Wu, W.J.; Garcia, E. Modeling the Effects of Electromechanical Coupling on Energy Storage through Piezoelectric Energy Harvesting. *IEEE-Asme Trans. Mechatron.* **2010**, *15*, 400–411. [[CrossRef](#)]
49. Bagheri, S.; Wu, N.; Filizadeh, S. Modeling of capacitor charging dynamics in an energy harvesting system considering accurate electromechanical coupling effects. *Smart Mater. Struct.* **2018**, *27*, 65026. [[CrossRef](#)]
50. Bagheri, S.; Wu, N.; Filizadeh, S. Numerical modeling and analysis of self-powered synchronous switching circuit for the study of transient charging behavior of a vibration energy harvester. *Smart Mater. Struct.* **2019**, *28*, 105056. [[CrossRef](#)]
51. Zhang, Z.W.; Xiang, H.J.; Tang, L.H. Modeling, analysis and comparison of four charging interface circuits for piezoelectric energy harvesting. *Mech. Syst. Signal Process.* **2021**, *152*, 107476. [[CrossRef](#)]
52. Yang, P.H.; Qu, X.P.; Liu, K.; Duan, J.J.; Li, J.; Chen, Q.; Xue, G.B.; Xie, W.K.; Xu, Z.M.; Zhou, J. Electrokinetic Supercapacitor for Simultaneous Harvesting and Storage of Mechanical Energy. *Acs Appl. Mater. Interfaces* **2018**, *10*, 8010–8015. [[CrossRef](#)] [[PubMed](#)]
53. Qian, W.Q.; Yang, W.Y.; Zhang, Y.; Bowen, C.R.; Yang, Y. Piezoelectric Materials for Controlling Electro-Chemical Processes. *Nano-Micro Lett.* **2020**, *12*, 149. [[CrossRef](#)] [[PubMed](#)]
54. Peddigari, M.; Park, J.H.; Han, J.H.; Jeong, C.K.; Jang, J.; Min, Y.; Kim, J.W.; Ahn, C.W.; Choi, J.J.; Hahn, B.D.; et al. Flexible Self-Charging, Ultrafast, High-Power-Density Ceramic Capacitor System. *Acs Energy Lett.* **2021**, *6*, 1383–1391. [[CrossRef](#)]
55. Xie, Y.Z.; Liu, Y.; Zhao, Y.D.; Tsang, Y.H.; Lau, S.P.; Huang, H.T.; Chai, Y. Stretchable all-solid-state supercapacitor with wavy shaped polyaniline/graphene electrode. *J. Mater. Chem. A* **2014**, *2*, 9142–9149. [[CrossRef](#)]
56. Wang, S.Y.; Dryfe, R.A.W. Graphene oxide-assisted deposition of carbon nanotubes on carbon cloth as advanced binder-free electrodes for flexible supercapacitors. *J. Mater. Chem. A* **2013**, *1*, 5279–5283. [[CrossRef](#)]

57. Pazhamalai, P.; Krishnamoorthy, K.; Mariappan, V.K.; Sahoo, S.; Manoharan, S.; Kim, S.J. A High Efficacy Self-Charging MoSe₂ Solid-State Supercapacitor Using Electrospun Nanofibrous Piezoelectric Separator with Ionogel Electrolyte. *Adv. Mater. Interfaces* **2018**, *5*, 1800055. [[CrossRef](#)]
58. Parida, K.; Bhavanasi, V.; Kumar, V.; Wang, J.X.; Lee, P.S. Fast charging self-powered electric double layer capacitor. *J. Power Sources* **2017**, *342*, 70–78. [[CrossRef](#)]
59. Song, R.B.; Jin, H.Y.; Li, X.; Fei, L.F.; Zhao, Y.D.; Huang, H.T.; Chan, H.L.W.; Wang, Y.; Chai, Y. A rectification-free piezo-supercapacitor with a polyvinylidene fluoride separator and functionalized carbon cloth electrodes. *J. Mater. Chem. A* **2015**, *3*, 14963–14970. [[CrossRef](#)]
60. Xing, L.L.; Nie, Y.X.; Xue, X.Y.; Zhang, Y. PVDF mesoporous nanostructures as the piezo-separator for a self-charging power cell. *Nano Energy* **2014**, *10*, 44–52. [[CrossRef](#)]
61. Maitra, A.; Karan, S.K.; Paria, S.; Das, A.K.; Bera, R.; Halder, L.; Si, S.K.; Bera, A.; Khatua, B.B. Fast charging self-powered wearable and flexible asymmetric supercapacitor power cell with fish swim bladder as an efficient natural bio-piezoelectric separator. *Nano Energy* **2017**, *40*, 633–645. [[CrossRef](#)]
62. He, H.X.; Fu, Y.M.; Zhao, T.M.; Gao, X.C.; Xing, L.L.; Zhang, Y.; Xue, X.Y. All-solid-state flexible self-charging power cell basing on piezo-electrolyte for harvesting/storing body-motion energy and powering wearable electronics. *Nano Energy* **2017**, *39*, 590–600. [[CrossRef](#)]
63. Xue, X.Y.; Deng, P.; Yuan, S.; Nie, Y.X.; He, B.; Xing, L.L.; Zhang, Y. CuO/PVDF nanocomposite anode for a piezo-driven self-charging lithium battery. *Energy Environ. Sci.* **2013**, *6*, 2615–2620. [[CrossRef](#)]
64. Xue, X.Y.; Deng, P.; He, B.; Nie, Y.X.; Xing, L.L.; Zhang, Y.; Wang, Z.L. Flexible Self-Charging Power Cell for One-Step Energy Conversion and Storage. *Adv. Energy Mater.* **2014**, *4*, 1301329. [[CrossRef](#)]
65. Pu, X.; Hu, W.G.; Wang, Z.L. Toward Wearable Self-Charging Power Systems: The Integration of Energy-Harvesting and Storage Devices. *Small* **2018**, *14*, 1702817. [[CrossRef](#)] [[PubMed](#)]
66. Luo, C.X.; Hu, S.H.; Xia, M.J.; Li, P.W.; Hu, J.; Li, G.; Jiang, H.B.; Zhang, W.D. A Flexible Lead-Free BaTiO₃/PDMS/C Composite Nanogenerator as a Piezoelectric Energy Harvester. *Energy Technol.* **2018**, *6*, 922–927. [[CrossRef](#)]
67. Lin, Z.H.; Yang, Y.; Wu, J.M.; Liu, Y.; Zhang, F.; Wang, Z.L. BaTiO₃ Nanotubes-Based Flexible and Transparent Nanogenerators. *J. Phys. Chem. Lett.* **2012**, *3*, 3599–3604. [[CrossRef](#)] [[PubMed](#)]
68. Wu, H.; Cui, Y. Designing nanostructured Si anodes for high energy lithium ion batteries. *Nano Today* **2012**, *7*, 414–429. [[CrossRef](#)]
69. Chan, C.K.; Peng, H.L.; Liu, G.; McIlwrath, K.; Zhang, X.F.; Huggins, R.A.; Cui, Y. High-performance lithium battery anodes using silicon nanowires. *Nat. Nanotechnol.* **2008**, *3*, 31–35. [[CrossRef](#)]
70. Lee, B.S.; Yoon, J.; Jung, C.; Kim, D.Y.; Jeon, S.Y.; Kim, K.H.; Park, J.H.; Park, H.; Lee, K.H.; Kang, Y.S.; et al. Silicon/Carbon Nanotube/BaTiO₃ Nanocomposite Anode: Evidence for Enhanced Lithium-Ion Mobility Induced by the Local Piezoelectric Potential. *ACS Nano* **2016**, *10*, 2617–2627. [[CrossRef](#)]
71. Su, X.; Wu, Q.L.; Li, J.C.; Xiao, X.C.; Lott, A.; Lu, W.Q.; Sheldon, B.W.; Wu, J. Silicon-Based Nanomaterials for Lithium-Ion Batteries: A Review. *Adv. Energy Mater.* **2014**, *4*, 1300882. [[CrossRef](#)]
72. Yada, C.; Ohmori, A.; Ide, K.; Yamasaki, H.; Kato, T.; Saito, T.; Sagane, F.; Iriyama, Y. Dielectric Modification of 5V-Class Cathodes for High-Voltage All-Solid-State Lithium Batteries. *Adv. Energy Mater.* **2014**, *4*, 1301416. [[CrossRef](#)]
73. Wen, L.; Wang, X.W.; Liu, G.Q.; Luo, H.Z.; Liang, J.; Dou, S.X. Novel surface coating strategies for better battery materials. *Surf. Innov.* **2018**, *6*, 13–18. [[CrossRef](#)]
74. Teranishi, T.; Yoshikawa, Y.; Sakuma, R.; Hashimoto, H.; Hayashi, H.; Kishimoto, A.; Fujii, T. High-rate performance of ferroelectric BaTiO₃-coated LiCoO₂ for Li-ion batteries. *Appl. Phys. Lett.* **2014**, *105*, 143904. [[CrossRef](#)]
75. Yoshikawa, Y.; Teranishi, T.; Hayashi, H.; Kishimoto, A. Loading effect of a barium titanate artificial interface on high voltage capabilities at high charge and discharge rates. *Jpn. J. Appl. Phys.* **2017**, *56*, 10pc01. [[CrossRef](#)]
76. Teranishi, T.; Inohara, M.; Kano, J.; Hayashi, H.; Kishimoto, A.; Yoda, K.; Motobayashi, H.; Tasaki, Y. Synthesis of nano-crystalline LiNbO₃-decorated LiCoO₂ and resulting high-rate capabilities. *Solid State Ion.* **2018**, *314*, 57–60. [[CrossRef](#)]
77. Takanashi, Y.; Orikasa, Y.; Mogi, M.; Oishi, M.; Murayama, H.; Sato, K.; Yamashige, H.; Takamatsu, D.; Fujimoto, T.; Tanida, H.; et al. Thickness estimation of interface films formed on Li_{1-x}CoO₂ electrodes by hard X-ray photoelectron spectroscopy. *J. Power Sources* **2011**, *196*, 10679–10685. [[CrossRef](#)]

Disclaimer/Publisher's Note: The statements, opinions and data contained in all publications are solely those of the individual author(s) and contributor(s) and not of MDPI and/or the editor(s). MDPI and/or the editor(s) disclaim responsibility for any injury to people or property resulting from any ideas, methods, instructions or products referred to in the content.